

# Dielectric properties of the system $\text{Ba}_{1-x}\text{La}_x\text{Ti}_{1-x}\text{Co}_x\text{O}_3$

O. PARKASH, C. DURGA PRASAD

*School of Materials Science and Technology, Institute of Technology,  
Banaras Hindu University, Varanasi-221 005, India*

D. KUMAR

*Department of Ceramic Engineering, Institute of Technology,  
Banaras Hindu University, Varanasi-221 005, India*

The dielectric behaviour of compositions with  $x = 0.01, 0.05, 0.10$  and  $0.20$  in the system  $\text{Ba}_{1-x}\text{La}_x\text{Ti}_{1-x}\text{Co}_x\text{O}_3$  was studied in the temperature range  $300\text{--}473$  K. The compositions with  $x = 0.01$  and  $0.05$  show a diffuse ferroelectric–paraelectric phase transition, while other compositions do not show this transition in this temperature range. The frequency dependence of dielectric constant and dielectric loss in the samples with  $x \geq 0.05$  indicates that space-charge polarization contributes significantly to their observed dielectric parameters.

## 1. Introduction

Most of the dielectrics used for ceramic capacitors have compositions based on barium titanate,  $\text{BaTiO}_3$ . Pure  $\text{BaTiO}_3$ , however, shows marked changes in the values of dielectric parameters with temperature, particularly near the Curie temperature. This is an undesirable feature for use as thermally stable capacitor materials. However,  $\text{BaTiO}_3$  offers a lot of flexibility by allowing a large number of substitutions at either Ba or Ti sites independently or simultaneously [1–3]. These substitutions are isovalent or heterovalent depending on whether the substituent ion has the same or a different valency from the ion to be substituted. For simultaneous heterovalent substitutions at Ba and Ti sites, a suitable combination of ions is necessary to maintain the electrical charge neutrality.

Recently we attempted to synthesize the system  $\text{Ba}_{1-x}\text{La}_x\text{Ti}_{1-x}\text{Co}_x\text{O}_3$  which represents the solid solution between  $\text{BaTiO}_3$  and  $\text{LaCoO}_3$ , with a view to studying the effect of simultaneous substitution of La and Co on the dielectric properties of  $\text{BaTiO}_3$  [4]. Although the effect of independent substitutions of La on Ba [5] and Co on Ti [6] sites, respectively, has been studied, no report is available as yet on the dielectric properties of this system where both ions are substituted simultaneously. The simultaneous substitution of  $\text{La}^{3+}$  for  $\text{Ba}^{2+}$  and  $\text{Co}^{3+}$  for  $\text{Ti}^{4+}$  leads to internal charge compensation in this system  $\text{Ba}_{1-x}\text{La}_x\text{Ti}_{1-x}\text{Co}_x\text{O}_3$ . Such a solid solution is termed as a valence-compensated solid solution. It has been found that single-phase materials form for all values of  $x \leq 0.50$  [4]. In this paper we report their dielectric behaviour. Similar studies on the preparation and dielectric properties of the analogous system  $\text{Pb}_{1-x}\text{La}_x\text{Ti}_{1-x}\text{Co}_x\text{O}_3$  have already been reported [7, 8].

## 2. Experimental procedure

Samples with  $x = 0.01, 0.05, 0.10, 0.20, 0.30$  and  $0.50$  were prepared by the ceramic method using  $\text{BaCO}_3$ ,  $\text{La}_2(\text{C}_2\text{O}_4)_3 \cdot n\text{H}_2\text{O}$ ,  $\text{Co}(\text{C}_2\text{O}_4)_2 \cdot 2\text{H}_2\text{O}$  and  $\text{TiO}_2$  all having purity better than 99.5%. The details of the method of preparation have been reported earlier [4]. Appropriate quantities of the constituent compounds were calcined at  $1473$  K in platinum crucibles for 4 h after thorough mixing. The calcined powders were mixed and ground again, and pressed as cylindrical pellets after the addition of appropriate quantities of 2% polyvinyl alcohol solution (PVA). Sintering of these pellets was done at  $1473$  K, as sintering at  $1573$  K resulted in the formation of a small amount of hexagonal  $\text{BaTiO}_3$  phase (5–10%) in the final product. The presence of Co in  $\text{BaTiO}_3$  is known to stabilize the hexagonal phase at lower temperatures [1]. Powder X-ray diffraction patterns were recorded for the final products using Ni-filtered  $\text{CuK}_\alpha$  radiation in a diffractometer (Jeol). The bulk density of these materials was determined by the water-displacement method, and the apparent porosity was calculated from the values of the true density and the bulk density. For the measurements of dielectric properties, the sintered pellets were polished, washed with isopropanol to remove any moisture and dried at  $423$  K overnight. Air-dried silver paint was applied on both surfaces, and again the pellets were left overnight at  $373$  K. Capacitance and dielectric loss,  $D$ , are measured as a function of temperature in the frequency range  $1$  kHz– $1$  MHz using an impedance analyser (Hewlett-Packard 4192A LF). Before taking observations, the entire cell assembly was heated to  $523$  K and cooled. All this care was taken to avoid the presence of any moisture. Any adsorbed moisture on  $\text{BaTiO}_3$  is known to influence dielectric properties significantly

[9]. Dielectric measurements were made only on the samples with  $x \leq 0.20$ . The compositions with  $x = 0.30$  and  $0.50$  were found to have significant conductivity at room temperature. For microstructural studies, fractured surfaces of sintered pellets were coated with gold and observed in a scanning electron microscope (Cambridge Stereoscan, model no. S4-10, UK).

### 3. Results and discussion

X-ray diffraction (XRD) data indicated the formation of single-phase materials in all the prepared samples. The composition with  $x = 0.01$  is tetragonal, similar to  $\text{BaTiO}_3$ , while all other samples have an overall cubic symmetry [4]. The presence of asymmetry in higher-angle diffraction lines of the compositions with  $x \geq 0.05$  indicates deviations from cubic symmetry in the local regions. This asymmetry decreases with increasing  $x$ . The bulk density and percentage porosity for various samples is given in Table I along with their structure and lattice parameters. Typical fractographs of some of the compositions are given in Fig. 1. The average grain size is in the range 2–3  $\mu\text{m}$ . In general, the grain size is small. This may partly be due to low sintering temperature and partly due to the effect of additives (La and Co).

Because of the smaller size (ionic radius,  $r = 0.122 \text{ nm}$ ) and different valency of  $\text{La}^{3+}$  as compared to  $\text{Ba}^{2+}$  ion ( $r = 0.146 \text{ nm}$ ), the substitution of  $\text{La}^{3+}$  for  $\text{Ba}^{2+}$  in the lattice will be associated with large elastic and electrostatic energy [10]. For similar

reasons to those discussed above, the presence of  $\text{Co}^{3+}$  for  $\text{Ti}^{4+}$  will be associated with a lot of elastic and electrostatic energy. Hence these  $\text{La}^{3+}$  and  $\text{Co}^{3+}$  ions will tend to segregate to the grain boundaries. The presence of these ions at grain boundaries will inhibit grain growth [5, 12].

The variation of dielectric constant,  $\epsilon$ , and dielectric loss,  $D$ , as a function of temperature for various compositions is shown in Figs 2–5. The sample with  $x = 0.01$  shows diffuse ferroelectric–paraelectric transition at 423 K (Fig. 2). The transition temperature remains the same at all three frequencies. The diffuseness of the transition increases in the sample with  $x = 0.05$ , and the  $\epsilon$  against  $T$  plot becomes almost flat (Fig. 3). The variation of its dielectric constant at 1 kHz within the temperature range 300–473 K is  $\sim 25\%$  of its value at 300 K. The variation decreases with increasing frequency.

Diffuse phase transition can arise due to (i) macroscopic inhomogeneities due to incomplete reactions during the preparation of these materials which are larger than the domain size [13]; (ii) stress and stress distribution induced by grain size (the diffuse phase transition observed in  $\text{BaTiO}_3$  for grain size  $< 1 \mu\text{m}$  has been explained on the basis of absence of  $90^\circ$  twinning in it [13]); (iii) microscopic inhomogeneities within one phase which extend over distances of the order of 5.0–100.0 nm [14, 15]. The inhomogeneities in this category are in thermodynamic equilibrium at high temperatures and may be frozen at low temperatures. These include compositional fluctuations, clustering and ordering etc., and related polarization.

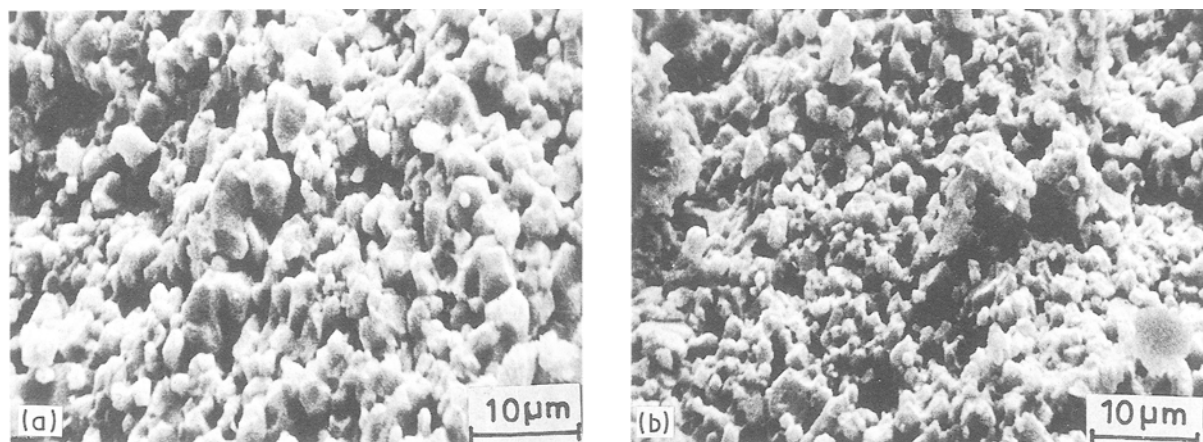


Figure 1 SEM of fractured surfaces of samples for (a)  $x = 0.01$  and (b)  $x = 0.05$ , in the system  $\text{Ba}_{1-x}\text{La}_x\text{Ti}_{1-x}\text{Co}_x\text{O}_3$ .

TABLE I Structure, lattice parameters, bulk density, percentage porosity and d.c. conductivity,  $\sigma_{\text{d.c.}}$  at 400 K for various samples in the system  $\text{Ba}_{1-x}\text{La}_x\text{Ti}_{1-x}\text{Co}_x\text{O}_3$

$x$	Lattice parameters			Bulk density ( $\text{g cc}^{-1}$ )	percentage porosity	$\sigma_{\text{d.c.}}$ ( $\Omega \text{ cm}^{-1}$ )
	Structure	$a(\text{nm})$	$c(\text{nm})$			
0.01	Tetragonal	0.3995	0.403	5.56	8.0	$1.63 \times 10^{-10}$
0.05	Cubic	0.3993	—	5.48	10.0	$1.40 \times 10^{-9}$
0.10	Cubic	0.3996	—	5.01	18.0	$1.57 \times 10^{-7}$
0.20	Cubic	0.3980	—	5.56	10.0	$4.00 \times 10^{-5}$

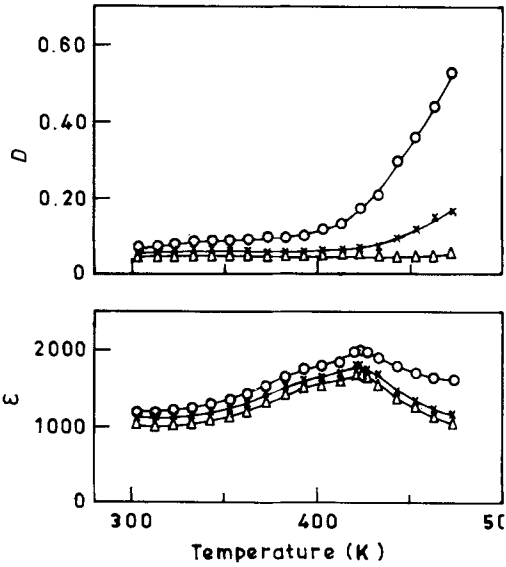


Figure 2 Variation of  $\epsilon$  and  $D$  with temperature for the sample with  $x = 0.01$  in the system  $\text{Ba}_{1-x}\text{La}_x\text{Ti}_{1-x}\text{Co}_x\text{O}_3$ .  $\circ$ , 1;  $\times$ , 10;  $\triangle$ , 100 kHz.

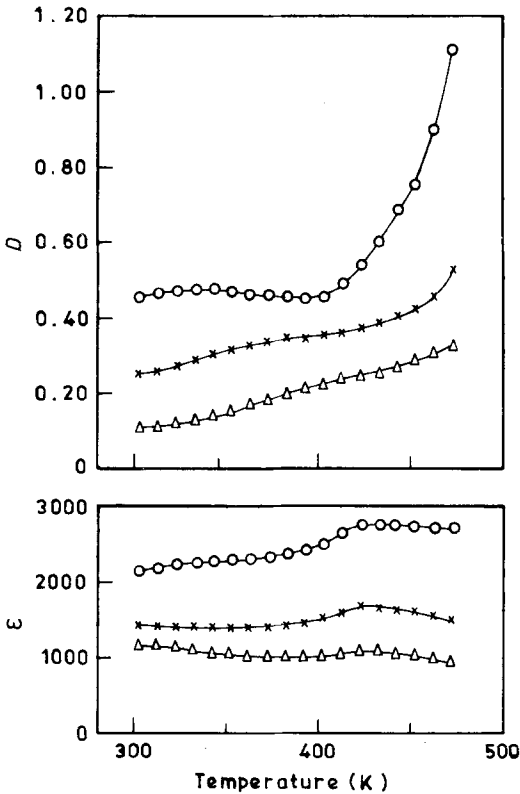


Figure 3 Variation of  $\epsilon$  and  $D$  with temperature for the sample with  $x = 0.05$  in the system  $\text{Ba}_{1-x}\text{La}_x\text{Ti}_{1-x}\text{Co}_x\text{O}_3$ .  $\circ$ , 1;  $\times$ , 10;  $\triangle$ , 100 kHz.

X-ray diffraction does not show any evidence for macroscopic inhomogeneities in these samples. Grain size is also not responsible for the diffuseness of the transition in the compositions with  $x = 0.01$  and  $0.05$ , as their average grain size is  $2\text{--}3\ \mu\text{m}$ . The diffuse nature of the transition is due to the presence of chemical heterogeneities present at the microlevel, because of the slow diffusion-controlled thermochemical ceramic process used for their preparation. Each micro-region will have its own Curie temperature determined by its composition. The overall behaviour

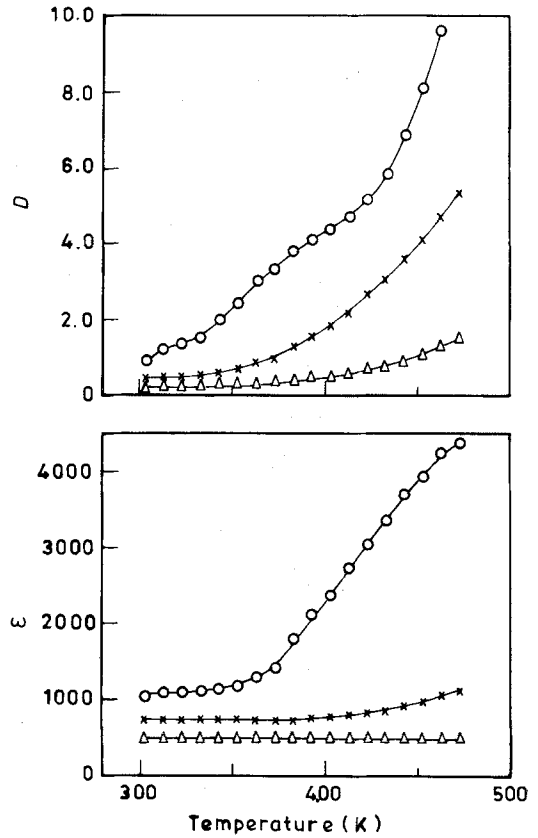


Figure 4 Variation of  $\epsilon$  and  $D$  with temperature for the sample with  $x = 0.10$  in the system  $\text{Ba}_{1-x}\text{La}_x\text{Ti}_{1-x}\text{Co}_x\text{O}_3$ .  $\circ$ , 1;  $\times$ , 10;  $\triangle$ , 100 kHz.

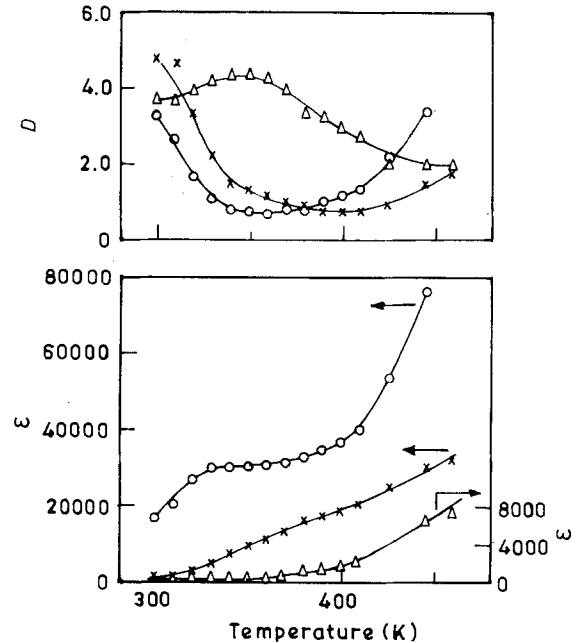


Figure 5 Variation of  $\epsilon$  and  $D$  with temperature for the sample with  $x = 0.20$  in the system  $\text{Ba}_{1-x}\text{La}_x\text{Ti}_{1-x}\text{Co}_x\text{O}_3$ .  $\circ$ , 1;  $\times$ , 10;  $\triangle$ , 100 kHz.

is the broad envelope of the behaviour of these different regions.

For the samples with  $x = 0.01$  and  $0.05$ , the dielectric constant,  $\epsilon$ , obeys the Curie-Weiss law:

$$\epsilon - 1 = \frac{C}{T - T_c} \quad (1)$$

above the Curie temperature at all the three frequencies namely 1, 10 and 100 kHz. Here  $C$  and  $T_c$  are known as Curie constant and Curie temperature, respectively. The Curie temperatures obtained from the  $\epsilon^{-1}$  against temperature plot at 1 kHz for  $x = 0.01$  and 0.05 are 387 and 397 K, respectively.

The compositions with  $x = 0.10$  and 0.20 do not show any anomaly in their  $\epsilon$  against  $T$  plots in the temperature range 300–473 K (Figs 4 and 5).  $\epsilon$  changes very little up to a particular temperature in the sample with  $x = 0.10$ . Thereafter it increases rapidly with temperature. The temperature coefficient of its dielectric constant decreases with increasing frequency. The sample with  $x = 0.20$  shows a very high value of dielectric constant, which is strongly frequency-dependent. The behaviour of dielectric loss is essentially similar to the compositions with  $x \leq 0.10$ . Initially,  $D$  varies very little with temperature and its variation becomes pronounced at high temperatures. The magnitude of  $D$  also increases with increasing  $x$ . This is due to increasing d.c. conductivity of these samples with increasing cobalt concentration (Table I) [16]. The variation of  $\epsilon$  and  $D$  with frequency for the samples with  $x = 0.01$  and 0.10 at a few temperatures is shown in Figs 6 and 7, respectively. Very little dispersion is observed in the  $\epsilon$  against  $\log f$  plots for the composition with  $x = 0.01$ . Behaviour of the samples with  $x = 0.05$  and 0.10 is essentially similar. The value of the dielectric constant decreases rapidly with increasing frequency up to 10 kHz and, thereafter the variation is very small at higher frequencies. The variation of dielectric loss with frequency is similar in all the three compositions with  $x \leq 0.10$ . It decreases sharply with increasing frequency. The frequency dependence is more pronounced at higher temperatures. For the composition with  $x = 0.20$ , a peak is observed in the  $D$  against  $\log f$  plot (Fig. 8). This peak shifts to higher frequency with increasing temperature. This may be due to relaxation of interfacial polarization. A peak in dielectric loss,  $D$  is observed when the relation

$$\omega\tau = 1 \quad (2)$$

is satisfied where  $\omega = 2\pi f$ ,  $f$  is the angular frequency, and  $\tau$  is the characteristic relaxation time. With increasing temperature,  $\tau$  decreases. This accounts for the shift of the peak in the  $D$  against  $\log f$  plot to

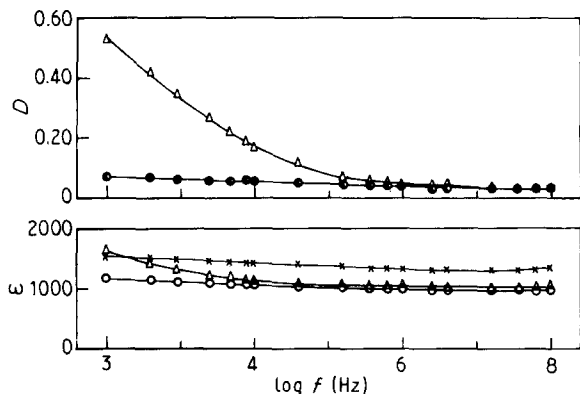


Figure 6 Variation of  $\epsilon$  and  $D$  with frequency at several temperatures for the sample with  $x = 0.01$ .  $\circ$ , 303;  $\times$ , 373;  $\triangle$ , 473 K.

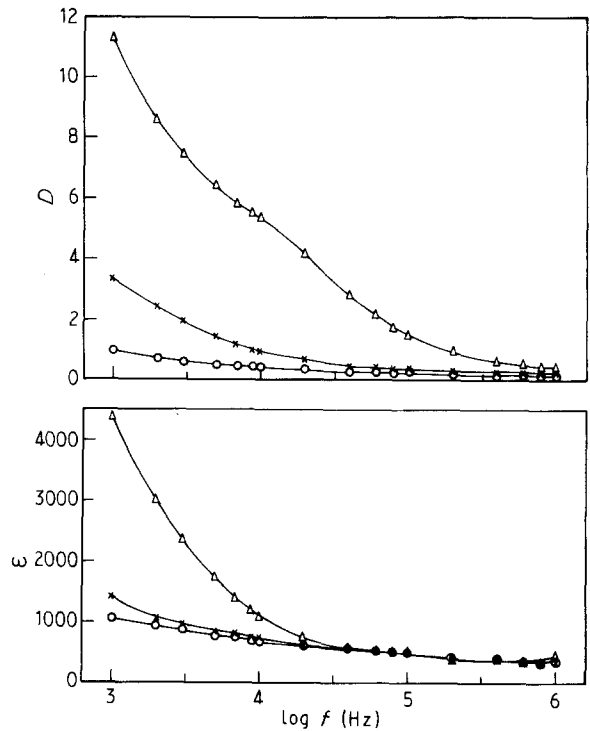


Figure 7 Variation of  $\epsilon$  and  $D$  with frequency at several temperatures for the sample with  $x = 0.10$ .  $\circ$ , 303;  $\times$ , 373;  $\triangle$ , 473 K.

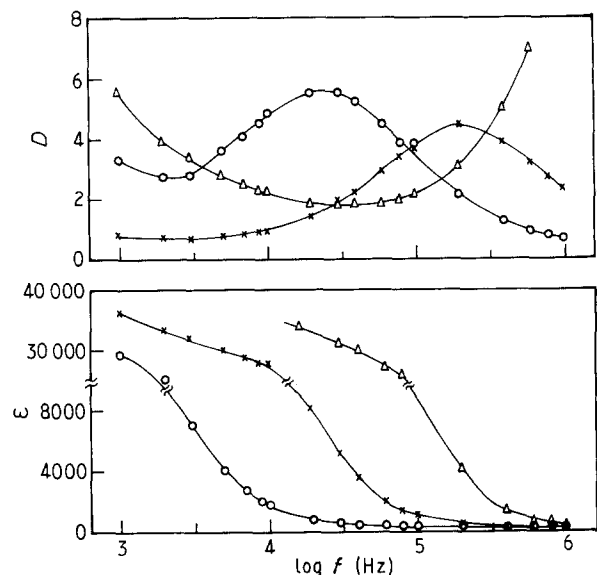


Figure 8 Variation of  $\epsilon$  and  $D$  with frequency at several temperatures for the sample with  $x = 0.20$ .  $\circ$ , 303;  $\times$ , 373;  $\triangle$ , 473 K.

higher frequency with increasing temperature, as observed experimentally in this composition.

The frequency dependence of  $\epsilon$  and  $D$  in these compositions indicates that interfacial polarization contributes significantly to their observed dielectric constant. The interfacial polarization cannot follow the rapidly changing electric field above  $\sim 10$  kHz which leads to a decrease in the value of  $\epsilon$  and  $D$ . Interfacial polarization arises due to random occupation of equivalent octahedral sites by Ti and Co, and of dodecahedral sites by Ba and La. This will give rise to micro-regions with different compositions, having different conductivities responsible for interfacial polarization. This is expected to increase with increasing

x. The observation of stronger frequency dependence of  $\epsilon$  and  $D$  with increasing  $x$  confirms this. The presence of these chemical heterogeneities at the micro-level also explains the diffuse nature of the phase transition in the compositions with  $x = 0.01$  and  $0.05$ , as mentioned above.

### Acknowledgements

Financial support from the Department of Science and Technology, Government of India, New Delhi, is gratefully acknowledged. We thank to Dr Lakshman Pandey for useful discussions.

### References

1. B. JAFFE, J. W. R. COOK and H. JAFFE, in "Piezoelectric Ceramics" (Academic, New York, 1971) Ch. 5.
2. R. NEWNHAM, *J. Mater. Educ.* **5** (1983) 941.
3. G. GOODMAN, in "Ceramics for Electronic Applications" edited by R. C. Buchanan (Marcel Dekker, New York, 1986) p. 90.
4. OM PARKASH, Ch. DURGA PRASAD and D. KUMAR, *J. Mater. Sci. Lett.* **8** (1989) 475.
5. K. S. MAZDYASNI and L. M. BROWN, *J. Amer. Ceram. Soc.* **54** (1971) 539.
6. T. SAKUDO, *J. Phys. Soc. Jpn* **12** (1957) 1050.
7. OM PARKASH, Ch. DURGA PRASAD and D. KUMAR, *J. Solid State Chem.* **69** (1987) 385.
8. *Idem.* *Phys. Status Solidi (a)* **106** (1988) 627.
9. A. J. MOUNTWALA, *J. Amer. Ceram. Soc.* **54** (1971) 544.
10. M. F. YAN, in "Microstructure and Properties of Ceramic Materials" edited by T. S. Yen and J. A. Park (Science Press, Beijing, 1984) p. 360.
11. A. TAWFIK and E. J. MEKAWY, *Ind. Ceram.* 811 (1986) 780.
12. D. HENNINGS and G. ROSENSTEIN, *J. Amer. Ceram. Soc.* **64** (1984) 249.
13. W. R. BUESSEM, L. E. CROSS and A. K. GOSWAMI, *ibid.* **49** (1966) 33.
14. G. A. SMOLENSKY, *J. Phys. Soc. Jpn* **28** (1970) 26.
15. V. A. ISUPOV and I. P. PRONIN, *ibid.* **B49** (1980) 53.
16. DEVENDRA KUMAR, Ch. DURGA PRASAD and OM PARKASH, *J. Phys. Chem. Solids* **51** (1990) 73.

*Received 10 April 1990  
and accepted 15 January 1991*